A Letters Journal Exploring the Frontiers of Physics

January 2020

EPL, **129** (2020) 24004 www.epljournal.org
doi: 10.1209/0295-5075/129/24004

Universality in the emergence of oscillatory instabilities in turbulent flows

Induja Pavithran[1], Vishnu R. Unni[2], Alan J. Varghese[3], R. I. Sujith[3], Abhishek Saha[2], Norbert Marwan[4] and Jürgen Kurths[4,5,6]

[1] *Department of Physics, IIT Madras - Chennai-600036, India*
[2] *Department of Mechanical and Aerospace Engineering, University of California - San Diego, CA, USA*
[3] *Department of Aerospace Engineering, IIT Madras - Chennai-600036, India*
[4] *Potsdam Institute for Climate Impact Research - Potsdam, Germany*
[5] *Department of Physics, Humboldt University - Berlin, Germany*
[6] *Institute for Complex Systems and Mathematical Biology, University of Aberdeen - Aberdeen, UK*

received 13 October 2019; accepted in final form 4 February 2020
published online 24 February 2020

PACS 43.28.Kt – Aerothermoacoustics and combustion acoustics
PACS 47.20.-k – Flow instabilities
PACS 47.53.+n – Fractals in fluid dynamics

Abstract – Self-organization driven by feedback between subsystems is ubiquitous in turbulent fluid mechanical systems. This self-organization manifests as emergence of oscillatory instabilities and is often studied in different system-specific frameworks. We uncover the existence of a universal scaling behaviour during self-organization in turbulent flows leading to oscillatory instability. Our experiments show that the spectral amplitude of the dominant mode of oscillations scales with the Hurst exponent of a fluctuating state variable following an inverse power law relation. Interestingly, we observe the same power law behaviour with a constant exponent near -2 across various turbulent systems such as aeroacoustic, thermoacoustic and aeroelastic systems.

Introduction. – A large number of physical systems involve turbulent flows that have chaotic variations in properties such as pressure and velocity. Turbulent flows are characterized by eddies of different length and time scales that interact nonlinearly. The transfer of energy across eddies of different length scales takes place through various cascade processes [1,2]. A unique collective behaviour can often arise from the interaction of multiple subsystems resulting in various phenomena at many different scales. Turbulent flow systems can therefore be regarded as a complex system. Although turbulent flows are chaotic, self-organization due to feedback in such a complex system can cause the emergence of order from chaos.

Self-organization is a fundamental property of a complex system, where some form of macroscopic order emerges from interactions between subsystems of an initially disordered system. In turbulent flows, spatially extended patterns such as large coherent structures are formed due to self-organization, for example, devastating cyclones in atmospheric flows. Self-organization driven by feedback between subsystems in turbulent systems can lead to oscillatory instabilities as observed in thermoacoustic [3], aeroacoustic [4], and aeroelastic systems [5]. These oscillatory instabilities cause high-amplitude vibrations which may incur catastrophic effects in engineering systems. In the present work, we study the emergence of such oscillatory instabilities in three different fluid mechanical systems, namely thermoacoustic, aeroacoustic, and aeroelastic systems.

Feedback between turbulent flow and other subsystems is often the cause for oscillatory instabilities. Thermoacoustic instability, a state of self-sustained large-amplitude periodic oscillations in the state variables, arises due to the nonlinear coupling between the reactive flow field and the acoustic field in a confinement [6]. This phenomenon can cause structural damages due to the increased thermal and vibrational loads, forcing shutdown of gas turbine engines [6,7], or failure of rockets [8]. Similarly, aeroacoustic instability is caused by the interaction between the acoustic field in a confinement and vortex shedding in turbulent flows [4]. Examples include the pleasant sounds generated in a flute or the destructive large-amplitude oscillations established in gas-transport pipelines [9]. Aeroelastic instability occurs as a consequence of the interaction

of the flow with the structural elements of the system [5], *e.g.*, the catastrophic collapse of the Tacoma Bridge [10]. The transition to such oscillatory instabilities from a state of chaotic oscillations in turbulent systems occurs via intermittency [11–13]. We attribute the emergence of ordered periodic oscillations from high-dimensional chaos to self-organization due to feedback between subsystems.

Conventionally, oscillatory instabilities in fluid mechanical systems are modeled as a transition from a stable fixed point to periodic oscillations (*i.e.*, Hopf bifurcation) as the control parameter is varied. According to linear theory, the amplitude grows exponentially during this transition, but then nonlinearities kick in and the amplitude saturates. In the study of such oscillatory instabilities, the effects of turbulence are often considered as background noise and are neglected in the traditional "signal plus noise" approach.

For turbulent flows, the stable operating point is never quiet, but is instead characterized by low amplitude fluctuations arising due to the presence of turbulence. Recently, for turbulent fluid mechanical systems, the stable operating state with aperiodic fluctuations was identified as high-dimensional deterministic chaos [14]. This state with underlying turbulent fluctuations possesses inherent complexity and multifractal characteristics [15,16]. Recent studies have shown that treating these fluctuations with their inherent complexities (as opposed to considering them as noise) is very rewarding in terms of obtaining precursors to such instabilities in practical application [11–13].

Further, a state of intermittency presages the self-sustained periodic oscillations in turbulent fluid mechanical systems [11–13]. The emergence of oscillatory instabilities in fluid mechanical systems may then be regarded as the loss of complexity in the dynamics [15,16]. Thus, considering the emergence of oscillatory instabilities from turbulence as a linear stability problem may not be the most appropriate and useful way, because every mode is already unstable in a turbulent system [17]. A more comprehensive way is to view the onset of oscillatory instabilities in a turbulent fluid mechanical system as order emerging from chaos using the framework of self-organization due to feedback between subsystems.

We explore the scaling behaviour of such self-organization leading to oscillatory instabilities in turbulent fluid mechanical systems. The proximity to the onset of oscillatory instability in each system is quantified using the Hurst exponent (H) which also serves as a system-independent parameter to study the scaling behaviour of self-organization. An unsteady variable of each of the three systems is measured as we vary an appropriate system-specific control parameter to approach oscillatory instability. We estimate H, which is related to the fractal dimension (D) as $H = 2 - D$, for the time series corresponding to each state [18].

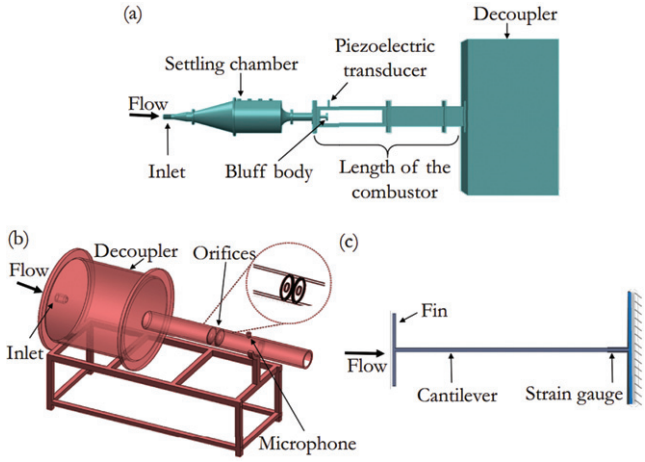

Fig. 1: Schematic of the experimental setups. (a) Turbulent combustor (thermoacoustic system) exhibiting transition to thermoacoustic instability. (b) An aeroacoustic system with two orifices. Vortices are shed when the turbulent flow passes through the orifices. In both of these systems, we measure the acoustic pressure fluctuations inside the duct during the transition to thermoacoustic/aeroacoustic instability. (c) An aeroelastic system where the left end of the beam has a small vertical fin attached to it. When a jet of air passes along the length of the cantilever from left to right, vortices are shed from the fins. We measure the resulting strain on the cantilever close to the fixed end of the beam. In all the cases, Reynolds number (Re) is varied as the control parameter to attain different dynamical states.

Experiments. – We analyze data from thermoacoustic, aeroacoustic and aeroelastic systems to study the transition from stable operation to oscillatory instabilities by changing the respective control parameters. In this section, we describe the experiments briefly. More details including the uncertainties of all measurements and the calculation of Reynolds number are provided in the Supplementary Material `Supplementarymaterial.pdf` (SM).

Experiments on thermoacoustic system. The schematic of the experimental setup is shown in fig. 1(a). The setup consists of a settling chamber, a burner, a flame holding device and a combustion chamber with variable duct length. The length of the combustion chamber is varied to achieve different acoustic length scales and timescales. Also, the combustor can be equipped with different flame stabilization mechanisms. The flame holding device (a bluff body or a swirl) is attached to the burner by a central shaft. Then, there is a sudden expansion from the circular burner to a square chamber. In this present work, data is presented for a bluff-body stabilized combustor for two lengths: 700 mm and 1400 mm. As opposed to this configuration, we also present data for a swirl stabilized combustor of length 700 mm. The two flame stabilizing mechanisms render completely different flow physics in the combustor leading to different mechanisms causing thermoacoustic

instability [19,20]. Liquified petroleum gas (LPG: butane 60% and propane 40% composition by mass) is used as the fuel. Air is partially premixed with LPG before the reactant mixture enters the combustion chamber. We ignite this fuel-air mixture using a spark plug. We decrease the equivalence ratio in order to attain different dynamical states in the system. The equivalence ratio is defined as $\phi = \frac{(\dot{m}_f/\dot{m}_a)_{actual}}{(\dot{m}_f/\dot{m}_a)_{stoichiometry}}$, where $\dot{m}_f$ and $\dot{m}_a$ are the mass flow rates of fuel and air, respectively. The mass flow rate of air is increased by keeping the mass flow rate of fuel constant to decrease ϕ.

As we approach thermoacoustic instability, the small vortices in turbulent reactive flows interact with each other, with the flame and with the acoustic field creating larger coherent structures. This emergent coherent dynamics in the flow field leads to the establishment of a coherent acoustic field which, in turn, affects the pattern of vortex shedding. Such alteration in the flow also changes the coupling between the subsystems. During thermoacoustic instability, the inter-subsystem interaction is very strong and a stable spatio-temporal pattern is formed due to self-organization, accompanied by large amplitude pressure oscillations [21]. The thermoacoustic data analyzed in this study are reported in Nair and Sujith [15], Nair *et al.* [11] and Unni and Sujith [22]. More detailed descriptions of the experiments can be found in these references.

The Reynolds number (Re) is considered as the control parameter and Re increases as we increase the mass flow rate of air. We choose a range of Re values for different configurations so as to achieve the transition from the low-amplitude aperiodic fluctuations to the high-amplitude limit cycle oscillations. For the bluff body stabilized combustor of length 700 mm (frequency of oscillations, $f \sim 250$ Hz), Re is varied from $(1.81 \pm 0.052) \times 10^4$ to $(2.8 \pm 0.073) \times 10^4$. For bluff body stabilized combustor of length 1400 mm ($f \sim 120$ Hz), Re varies from $(1.96 \pm 0.006) \times 10^4$ to $(3.53 \pm 0.099) \times 10^4$. Re variation for swirl stabilized combustor (length = 700 mm and $f \sim 250$ Hz) is from $(1.61 \pm 0.041) \times 10^4$ to $(1.96 \pm 0.060) \times 10^4$. The unsteady pressure fluctuations inside the combustion chamber are measured using piezoelectric transducers at different values of Re in the above-mentioned ranges. The transducer is located at the antinode of pressure oscillations which is near the backward facing step. This location helps us to record the maximum amplitude of the standing wave. The pressure data is sampled at a rate of 10 kHz.

Experiments on aeroacoustic system. Another fluid mechanical system exhibiting oscillatory instability arising out of a turbulent flow field is an aeroacoustic system. Typically, it consists of orifices located inside a duct. Vortices are shed when the turbulent flow passes through the orifices. The interaction between the vortex shedding and the acoustics inside the duct determines the dynamics of the aeroacoustic system. The schematic of the aeroacoustic experimental setup is shown in fig. 1(b). The current experimental setup consists of a cylindrical chamber, two pipes (lengths: 300 mm and 225 mm, respectively), and two circular orifices of diameter 20 mm each, thickness 2.5 mm and separated by a distance of 18 mm (a zoomed view is shown in the circle). The turbulent flow enters the pipe through the large cylindrical chamber, referred to as the decoupler, which isolates the duct from the upstream pressure fluctuations. Thus, the pressure at both ends of the duct is maintained at the ambient pressure. The experiments are conducted by increasing the Re from 5615 ± 185 to 9270 ± 212. Here, f varies from 484 Hz to 540 Hz as we increase the velocity of the inlet flow. We measure the pressure fluctuations inside the duct at a distance of 100 mm from the second orifice. The data is sampled at a rate of 10 kHz.

Experiments on aeroelastic system. In a similar manner, we study the transition to aeroelastic instability in a laboratory scale aeroelastic system (fig. 1(c)). The experimental setup consists of a cantilever beam having 45 mm length, 25 mm width and 0.5 mm thickness. The right side of the beam is fixed, and the left side of the beam is free. Note that the left end of the beam has a small vertical fin (12 mm length) attached to it, akin to a winglet of an aircraft wing. When a jet of air passes along the length of the cantilever from left to right, vortices are shed from the fins. These vortices impart unsteady aerodynamic load to the cantilever. We measure the resulting strain on the cantilever close to the fixed end of the beam (5 mm from the fixed end), using a strain gauge. For particular flow rates, the oscillations in the cantilever beam become periodic and self-sustained, resulting in aeroelastic instability. Here, we increase Re from 2384 ± 159 to 4768 ± 111 to capture the transition to aeroelastic instability ($f \sim 60$ Hz). We record the strain data corresponding to the structural vibrations in the system for different values of the control parameter.

Results. – We analyze the time series of acoustic pressure fluctuations during the transition to oscillatory instabilities for thermoacoustic and aeroacoustic systems. In the case of the aeroelastic system, we analyze the time series of strain experienced by the structure. In this work, we study the transition to oscillatory instabilities in the following different cases: i) a bluff body stabilized combustor of length 700 mm, ii) and one of length 1400 mm, iii) a swirl stabilized combustor of length 700 mm, iv) an aeroacoustic system and v) an aeroelastic system. We choose these systems as they have different mechanisms for onset of oscillatory instability and have different levels of turbulence, amplitude and frequency of oscillations. The first three cases are for thermoacoustic system and in the first two cases, the length of the combustor is varied to achieve different acoustic timescales. Similarly, different flame stabilizing mechanisms are used to generate different mechanisms leading to oscillatory instability.

In fig. 2, we show representative datasets from all the three systems.

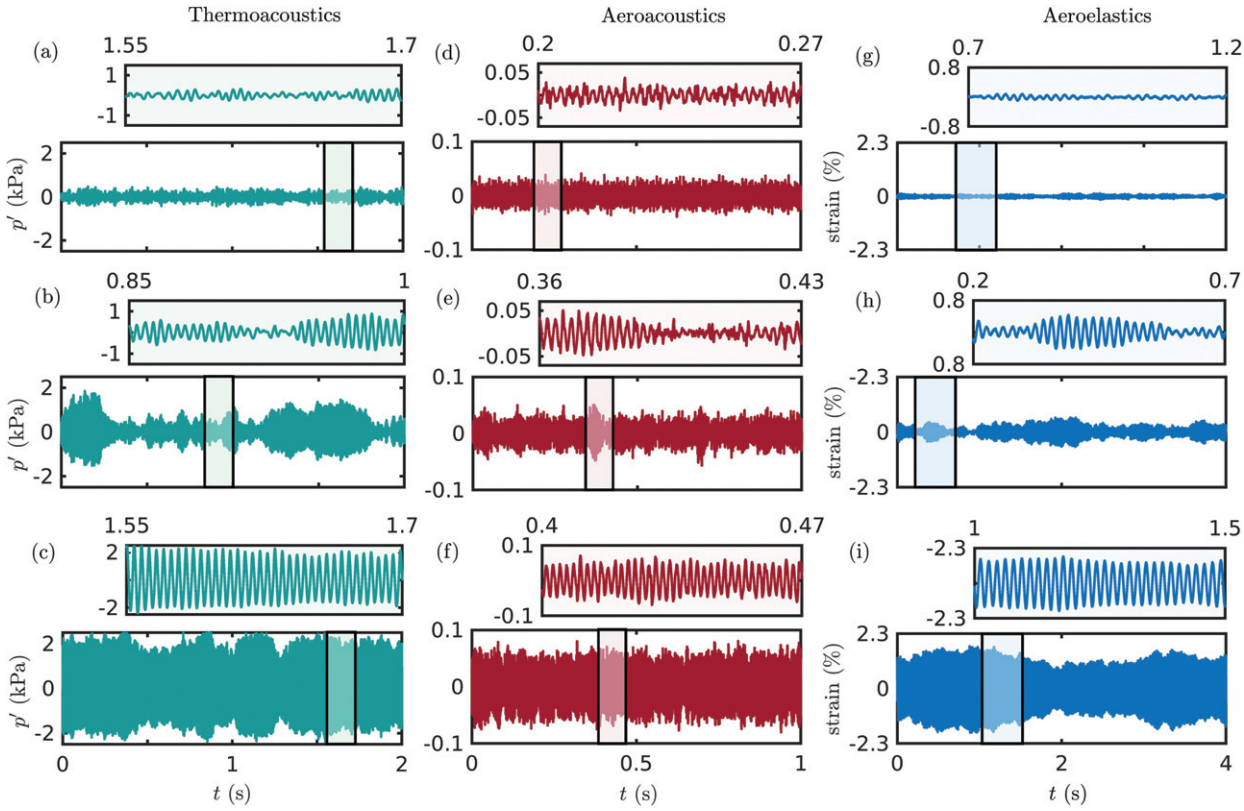

Fig. 2: Time series of state variables during the transition to oscillatory instability. (a)–(c) Data representing the acoustic pressure fluctuations acquired from a bluff body stabilized combustor of length 700 mm. The corresponding Re for (a), (b) and (c) are $(1.9 \pm 0.053) \times 10^4$, $(2.6 \pm 0.069) \times 10^4$ and $(2.8 \pm 0.073) \times 10^4$, respectively. (d)–(f) Acoustic pressure fluctuations acquired during the transition to aeroacoustic instability ($Re = 5615 \pm 185$, 7283 ± 198 and 9270 ± 212 corresponding to (d), (e) and (f)). (g)–(i) The time series of strain experienced by the cantilever in the aeroelastic system as we vary Re (2384 ± 111, 3972 ± 142 and 4768 ± 159). In all the systems, we observe a transition from low-amplitude aperiodic fluctuations ((a), (d) and (g)) to high-amplitude periodic oscillations ((c), (f) and (i)) via a regime of intermittency where intermittent bursts of high-amplitude periodic oscillations appear in a nearly random fashion amidst epochs of low-amplitude aperiodic fluctuations ((b), (e) and (h)) as we vary the control parameters (Re increases from top to bottom). The transition from aperiodicity to periodicity always occurs via a regime of intermittency for other configurations of these systems as well.

I) Figure 2(a)–(c) shows the acoustic pressure fluctuations in a thermoacoustic system (case i)) during the transition to thermoacoustic instability. Figure 2(a) corresponds to a chaotic state far from the oscillatory instability. The time series consists of low-amplitude aperiodic fluctuations. Recently, Tony *et al.* [14] showed that these aperiodic fluctuations have features of high-dimensional chaos contaminated with white and coloured noise. Nair *et al.* [11] discovered that the transition to thermoacoustic instability occurs through a state of intermittency, which contains epochs of high-amplitude periodic oscillations amidst low-amplitude aperiodic oscillations (fig. 2(b)). Thermoacoustic instability (fig. 2(c)) corresponds to a state of high-amplitude periodic oscillations. We observe a similar behaviour for all the above-mentioned combustor configurations during the transition to thermoacoustic instability.

II) Figure 2(d)–(f) shows the time series of pressure fluctuations corresponding to the transition to aeroacoustic instability. The temporal behaviour of acoustic pressure during this transition is similar to that in the thermoacoustic system, despite the fact that the amplitude levels in both systems differ by orders of magnitude.

III) Figure 2(g)–(i) represents the time series of strain experienced by the structure during the transition to aeroelastic instability. The observed oscillations are similar to those of the thermoacoustic and aeroacoustic systems, even though we are measuring a completely different unsteady variable.

From fig. 2, we clearly see that these turbulent systems considered here follow an intermittency route to oscillatory instability. We observe a similar transition in all the three classes of systems even though the interacting subsystems and the physical mechanisms involved are different.

Next, we quantify the proximity to the onset of oscillatory instability in the discussed systems using the Hurst

exponent (H). As mentioned earlier, the periodic content in time series of the unsteady variable increases as we approach an oscillatory instability. The state of low-amplitude aperiodic oscillations has a fractal nature which is born out of the inherent fractal nature of turbulence. As the system self-organizes into oscillatory instability, the fractal time series transitions to a more regular periodic signal [15]. We capture the variation of fractal characteristics of the time series by calculating H following the multifractal detrended fluctuation analysis (detailed in the SM).

The Hurst exponent represents the scaling of the *rms* of the standard deviation of fluctuations with the scale size or the time interval considered for obtaining the fluctuations. Generally, H has values between 0 and 1 for time series (*i.e.*, fractal dimension between 1 and 2). It provides a measure of persistence in a time series. For a persistent time series wherein subsequent values are highly correlated, $H > 0.5$. An antipersistent signal has $H < 0.5$, in which a high value of the signal is most likely followed by a low value. $H = 0.5$ corresponds to an uncorrelated random process.

In our analysis, we compute H for the time series corresponding to the unsteady variable obtained at each state during the transition to oscillatory instability in thermoacoustic, aeroacoustic and aeroelastic systems. H for each state is calculated from the time series divided into segments of selected duration. The choice of the range of scale (or segment length) should be optimal to capture the transition from an aperiodic to a periodic state [23]. The periodicity at the onset of oscillatory instability will not be captured if we select segments of the length corresponding to less than one cycle of oscillation. Further, the fluctuations will be averaged out if we choose segments with a large number of cycles. Therefore, we choose two to four cycles of oscillations during the periodic regime as the optimum scale.

In fig. 3, we plot the amplitude of the dominant mode of oscillations (A) and the Hurst exponent (H) for the time series of pressure oscillations as a function of Reynolds number (Re) for the thermoacoustic system (described earlier as case i)). Note that A is the amplitude of the dominant peak from the amplitude spectrum of the fluctuating state variable obtained using the fast Fourier transform. The signal corresponding to thermoacoustic instability has H very close to 0, as the signal is perfectly periodic. We observe that during the transition, A increases steeply near the onset of thermoacoustic instability as we vary the control parameter. In contrast, H gradually decreases towards zero during the transition. The amplitude of oscillations or the value of A at the onset of oscillatory instability depends on the specific system under consideration. On the other hand, the variation of H describes the self-organization in turbulent flows into oscillatory instabilities, independent of the system features.

We plot the variation of A/A_I with H in log-log scale (fig. 4) for the five different cases mentioned earlier. Here, we normalize A of each system with the amplitude of

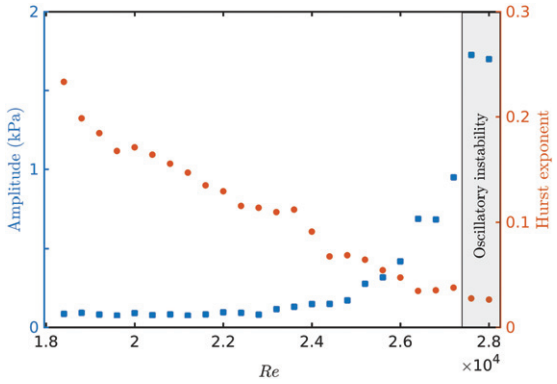

Fig. 3: Amplitude of the dominant mode of oscillations and the Hurst exponent for unsteady pressure signals as a function of Reynolds number (Re). We analyze the data from a laboratory bluff body stabilized combustor of length 700 mm for different Re. The amplitude is obtained from the amplitude spectrum plotted with a resolution of 4 Hz. The amplitude increases steeply near the transition to thermoacoustic instability, whereas the Hurst exponent shows a gradual decrease during the transition and is approaching zero.

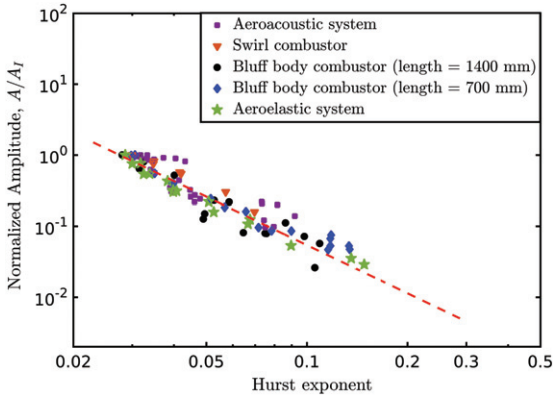

Fig. 4: Inverse power law scaling of amplitude with Hurst exponent. Variation of amplitude with Hurst exponent is plotted on a logarithmic scale for the data acquired from different systems. We observe a power law relation with a constant power law exponent around -2.

oscillations at the onset of instability (A_I) for the given system. We observe that all the data points collapse to a single straight line and this reveals an inverse power law relation between A and H during the intermittency regime. For all the data irrespective of the frequency of oscillations or the physics of the system, the experimentally observed value for the power law exponent is found to remain constant around -2 (-1.83 ± 0.17 for the bluff body combustor with length 700 mm, -2.22 ± 0.58 for the bluff body combustor with length 1400 mm, -2.06 ± 0.24 for the swirl combustor, -2.02 ± 0.32 for the aeroacoustic system and -2.21 ± 0.19 for the aeroelastic system). The uncertainties are estimated for 90% confidence intervals. The points with $H > 0.1$ are ignored while finding the power law exponent as they represent the low-amplitude aperiodic oscillations far away from the self-organized state.

Scaling laws and universality are important concepts in statistical physics. They describe the striking similarity in the behaviour during critical transitions among systems that are otherwise different. Scaling in non-equilibrium phase transitions has been a topic of interest in recent years [24]. For example, Tham *et al.* [25] experimentally obtained a similar power law scaling relationship between the electrostatic fluctuation levels and the linear growth rate for self-organization in turbulent plasma leading to a quasi-coherent state.

Discussions. – Transition to oscillatory instability in the class of turbulent fluid mechanical systems discussed here occurs via the state of intermittency and we observe a universal scaling law during the transition. In fluid dynamics literature, intermittency refers to a state in which a laminar flow is interrupted by high-amplitude turbulent bursts at apparently random intervals [26]. During the bursts, the phase space trajectory goes to a larger chaotic attractor with the original periodic attractor as its subset. Three types of bifurcations are associated with such intermittencies, namely, cyclic fold, subcritical Hopf, and subcritical period-doubling bifurcations. Intermittencies corresponding to these bifurcations are labelled as type I, II and III, respectively [27,28][1].

In our case, to begin with, the system is chaotic and is Lyapunov stable. However, during intermittency, this stability is lost and the system intermittently approaches limit cycle oscillations. In contrast to the known types of intermittencies discussed above, here, the intermittency comprises high-amplitude periodic oscillations amidst epochs of low-amplitude aperiodic oscillations [30]. The trajectory in the phase space goes to a larger periodic attractor from a smaller chaotic attractor during the intermittent bursts (fig. 2(b), (e) and (h)). Thus, there is an inherent difference in the type of intermittency observed during the emergence of oscillatory instabilities in turbulent flows, as observed for example in thermoacoustic, aeroacoustic and aeroelastic systems compared to the classical ones.

In the present study, we observe the scaling behaviour in all the systems we have examined, where oscillatory instabilities emerge in turbulent flows. We do not observe this inverse power law relation in models such as kicked oscillator [31] or noisy Hopf bifurcations [32], even though they capture the transition from chaos to limit cycle via intermittency. Further, this scaling is not exhibited by models which capture the transition from chaos to periodic oscillations through type I, II and III intermittencies (shown in the SM). This experimentally observed scaling appears to be a universal property for a class of systems in which order emerges from chaos, as a result of self-organization in turbulence following an intermittency route.

Fully developed, isotropic turbulence has a well-known power law scaling for its energy spectrum [1,2], which shows the distribution of energy across different wave numbers. The instances of self-organization in turbulence leading to oscillatory instability discussed in this paper are associated with the emergence of periodically shed, large coherent structures in the flow. This emergence of oscillatory instability is accompanied by the redistribution of energy across different length scales and thus deviation from the scaling observed in fully developed turbulent flows. In the various systems which we examine, as we approach oscillatory instabilities by changing some control parameter of each system, the redistribution of energy into the most dominant scale (*i.e.*, scale of coherent structure) in each system is captured by studying the amplitude spectra of an appropriate state variable of the system. In our study, we used unsteady pressure measurements for thermoacoustic and aeroacoustic systems and strain rate for the aeroelastic system.

Oscillatory instabilities in engineering systems such as rocket engines, power-producing gas turbine engines, gas transport pipelines and swaying skyscrapers are undesirable and can produce ruinously high-amplitude vibrations with catastrophic consequences. Using this scaling between H and A, we predict the amplitude of oscillations well before the onset of oscillatory instability using the data points obtained during the stable operation [33]. This *a priori* estimation of amplitude helps in devising strategies to mitigate such oscillatory instabilities and also helps save a lot of money involved in testing the hardware.

Conclusions. – In the present study, using three different systems, we describe a universal route through which oscillatory instabilities emerge in turbulent flow. The amplitude of the dominant mode of oscillations increases following an inverse power law scaling with the Hurst exponent of the time series of the appropriate state variable, and the scaling exponent is invariant across the three systems considered. The proximity to the onset of oscillatory instabilities is quantified by the Hurst exponent, which serves as a system-independent measure of self-organization. Here, the spectral amplitude of the dominant mode of oscillations serves as the order parameter of the system.

Power law scaling relations have been discovered for various critical transitions. Here, we report the experimental observation of a scaling behaviour ($A \propto H^{-2}$) for a class of non-equilibrium systems. The discovery of this unique scaling enables *a priori* estimation of the amplitude of oscillations at the onset of oscillatory instability. This information on the amplitude can be critical in devising the countermeasures needed to limit the possible damages from such oscillatory instabilities.

* * *

We express our gratitude to the Department of Science and Technology, Government of India for providing financial support under the grant Nos.: DST/SF/1(EC)/2006

[1]Several other types of intermittencies have been reported and discussed [29].

(Swarnajayanti Fellowship) and JCB/2018/000034/SSC (JC Bose Fellowship). We acknowledge the discussions and help from Dr. G. Thampi, Dr. V. Nair, Mr. Manikandan R, Mr. Thilagraj and Mr. Anand. IP is indebted to Ministry of Human Resource Development, India and Indian Institute of Technology Madras for providing research assistantship.

REFERENCES

[1] Richardson L. F., *Proc. R. Soc. London Ser. A*, **110** (1926) 709.
[2] Kraichnan R. H., *Phys. Fluids*, **10** (1967) 1417.
[3] Juniper M. P. and Sujith R., *Annu. Rev. Fluid Mech.*, **50** (2018) 661.
[4] Flandro G. A. and Majdalani J., *AIAA J.*, **41** (2003) 485.
[5] Hansen M. H., *Wind Energy*, **10** (2007) 551.
[6] Lieuwen T. C. and Yang V., *Combustion Instabilities in Gas Turbine Engines: Operational Experience, Fundamental Mechanisms, and Modeling* (American Institute of Aeronautics and Astronautics) 2005.
[7] Fleming C., *Wall Street Journal* (February 13, 1998).
[8] Fisher S. C. and Rahman S. A., *Remembering the Giants: Apollo Rocket Propulsion Development*, *NASA Monographs in Aerospace History series* (NASA) 2009.
[9] Kriesels P. C., Peters M., Hirschberg A., Wijnands A., Iafrati A., Riccardi G., Piva R. and Bruggeman J. C., *J. Sound Vib.*, **184** (1995) 343.
[10] Larsen A. and Walther J. H., *J. Wind Eng. Ind. Aerodyn.*, **67** (1997) 253.
[11] Nair V., Thampi G. and Sujith R. I., *J. Fluid Mech.*, **756** (2014) 470.
[12] Nair V. and Sujith R. I., *Int. J. Aeroacoust.*, **15** (2016) 312.
[13] Venkatramani J., Nair V., Sujith R. I., Gupta S. and Sarkar S., *J. Fluids Struct.*, **61** (2016) 376.
[14] Tony J., Gopalakrishnan E. A., Sreelekha E. and Sujith R. I., *Phys. Rev. E*, **92** (2015) 062902.
[15] Nair V. and Sujith R. I., *J. Fluid Mech.*, **747** (2014) 635.
[16] Venkatramani J., Nair V., Sujith R. I., Gupta S. and Sarkar S., *J. Sound Vib.*, **386** (2017) 390.
[17] Huhn F. and Magri L., *J. Fluid Mech.*, **882** (2020) A24.
[18] Mandelbrot B. B., *The Fractal Geometry of Nature*, Vol. **1** (W.H. Freeman, New York) 1982.
[19] Ghoniem A. F., Park S., Wachsman A., Annaswamy A., Wee D. and Altay H. M., *Proc. Combust. Inst.*, **30** (2005) 1783.
[20] Steinberg A. M., Boxx I., Stöhr M., Carter C. D. and Meier W., *Combust. Flame*, **157** (2010) 2250.
[21] George N. B., Unni V. R., Raghunathan M. and Sujith R. I., *J. Fluid Mech.*, **849** (2018) 615.
[22] Unni V. R. and Sujith R. I., *J. Fluid Mech.*, **784** (2015) 30.
[23] Kerres B., Nair V., Cronhjort A. and Mihaescu M., *SAE Int. J. Eng.*, **9** (2016) 1795.
[24] Täuber U. C., *Annu. Rev. Condens. Matter Phys.*, **8** (2017) 185.
[25] Tham P. and Sen A. K., *Phys. Rev. Lett.*, **72** (1994) 1020.
[26] Nayfeh A. H. and Balachandran B., *Applied Nonlinear Dynamics: Analytical, Computational, and Experimental Methods* (Wiley Interscience, New York) 2008.
[27] Manneville P. and Pomeau Y., *Phys. Lett. A*, **75** (1979) 1.
[28] Pomeau Y. and Manneville P., *Commun. Math. Phys.*, **74** (1980) 189.
[29] Schuster H. G. and Just W., *Deterministic Chaos: An Introduction* (John Wiley & Sons) 2006.
[30] Pawar S. A. and Sujith R. I., *Intermittency: A State that Precedes Thermoacoustic Instability*, in *Droplets and Sprays* (Springer) 2018, p. 403.
[31] Seshadri A., Nair V. and Sujith R. I., *Combust. Theory Model.*, **20** (2016) 441.
[32] Noiray N., *J. Eng. Gas Turbines Power*, **139** (2017) 041503.
[33] Pavithran I., Unni V. R. and Sujith R. I., Patent of Addition to U.S. Patent No. US20150260609A1 (Priority date: 23 July 2018).